

Graphene-based quantum heterospin graphs

Gabriel Martínez-Carracedo^{1,2}, Amador García-Fuente^{1,2},

László Oroszlány^{3,4}, László Szunyogh^{5,6}, and Jaime Ferrer^{1,2}

¹*Departamento de Física, Universidad de Oviedo, 33007 Oviedo, Spain*

²*Centro de Investigación en Nanomateriales y Nanotecnología,
Universidad de Oviedo-CSIC, 33940, El Entrego, Spain*

³*Department of Physics of Complex Systems, Eötvös Loránd University, 1117 Budapest, Hungary*

⁴*Wigner Research Centre for Physics, H-1525, Budapest, Hungary*

⁵*Department of Theoretical Physics, Institute of Physics,
Budapest University of Technology and Economics, Műegyetem rkp. 3., H-1111 Budapest, Hungary*

⁶*HUN-REN-BME Condensed Matter Research Group,
Budapest University of Technology and Economics,
Műegyetem rkp. 3., H-1111 Budapest, Hungary*

We investigate from first principles a variety of low-dimensional open quantum spin systems based on magnetic nanographene structures that contain spin-1/2 and spin-1 triangulenes and/or olympicenes. These graphene nanostructures behave as localized spins and can be effectively described by a quantum bilinear-biquadratic Heisenberg Hamiltonian, for which we will compute the energy spectrum and the quantum numbers associated with the low-energy eigenstates. We propose the experimental realization of antiferromagnetic alternating spin chains using these graphene nanostructures, which result in ferrimagnetic systems whose ground state spin and degeneracy depend on the length of the chain. We also identify a double degeneracy in the total spin quantum number S in the first excited state for three-leg spin graphs (3-LSGs). This degeneracy depends on both the number of sites and the spin species that compose the 3-LSG. We identify the double degeneracy of the first excited state as a consequence of swapping transformation symmetry of the Hamiltonian.

I. INTRODUCTION

Harnessing quantum-regime functionalities without relying on rare-earth elements represents a significant step toward the development of globally-sourced and more accessible quantum technologies. Moreover, implementing using widely accessible materials, such as graphene-based devices [1–4] or other molecular systems [5], has garnered significant attention from both theorists and experimentalists. Quantum spin systems provide an excellent playground for exploring the physical properties of strongly correlated systems [6, 7] and they can be used to construct platforms for quantum computing [8]. Some examples of spin quantum systems include two-dimensional magnets [9–12], quantum dots [13, 14] or topological spin textures [15, 16]. In this paper, we focus on specific magnetic nanographene structures [17–20] and use them as magnetic building blocks (MBBs) to construct various interacting spin systems. This is because these MBBs possess a magnetic moment whose magnitude is determined by Lieb’s theorem [21], taking into account the imbalance of carbon atoms in each sublattice. We focus on three MBBs that have already been synthesized experimentally: the spin-1 triangulene (S-1T) [22], the spin-1/2 olympicene (S-1/2O) [23], and the spin-1/2 triangulene (S-1/2T) [24], which are circled in blue in Figs. 1(a-c). Since their magnetic moments are sufficiently localized and fixed, and there is no source of anisotropy, the interaction between MBBs can be appropriately described by an isotropic quantum Heisenberg Hamiltonian. It has been shown that to describe effectively the exchange in-

teraction between MBBs in these graphene nanostructures a biquadratic interaction [25, 26] must be included. The bilinear-biquadratic (BLBQ) Hamiltonian reads

$$\hat{H}_{\text{BLBQ}} = \frac{1}{2} \sum_{i \neq j} J_{ij} \left(\hat{\mathbf{S}}_i \cdot \hat{\mathbf{S}}_j + \beta_{ij} \left(\hat{\mathbf{S}}_i \cdot \hat{\mathbf{S}}_j \right)^2 \right) \quad (1)$$

where $\hat{\mathbf{S}}_i = (\hat{S}_i^x, \hat{S}_i^y, \hat{S}_i^z)$ is a vector whose components are the spin- S operators in the x , y , and z directions for the i th MBB. Note that for each site i , the spin operator may differ (either spin-1 or spin-1/2) depending on the type of MMB associated with i . J is the isotropic exchange constant and β is a parameter that modulates the biquadratic exchange interaction.

In this paper, we present an AB-INITIO study that combines the exact diagonalization (ED) method [27, 28] with density functional theory (DFT) and the LKAG formalism to extract information about the energy gaps and state degeneracies of multi-legged spin systems described by Eq. 1. The structure of the paper is as follows. In Section II, we explain the method used to characterize the nanographene spin structures. In Section III, we present the results for alternating spin chains, three-leg spin graphs (3-LSGs). In this section, we also discuss and characterize the degeneracy that arises in 3-LSGs when a swapping symmetry group isomorphic to the C_{3v} point group is present. Finally, we summarize the results and present our conclusions in Section IV.

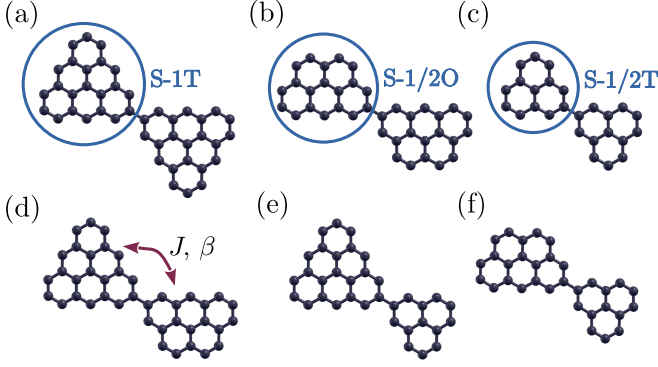


FIG. 1. (a-f) Magnetic dimer systems coupled by bilinear J and biquadratic β exchange constants. These dimers are composed of different graphene-based MBBs: S-1T, S-1/2T, and S-1/2O. The dimers are: (a) S-1T and S-1T, (b) S-1/2O and S-1/2O, (c) S-1/2T and S-1/2T, (d) S-1T and S-1/2O, (e) S-1T and S-1/2T, and (f) S-1/2O and S-1/2T.

II. COMPUTATIONAL METHOD

We follow a three-step procedure to study and characterize these magnetic graphene-based nanostructures. The first step is to compute the electronic Hamiltonian for the various dimer systems depicted in Fig. 1 using Density Functional Theory (DFT) [29, 30] via the SIESTA code [31]. For the SIESTA calculations, we employed the Generalized Gradient Approximation (GGA) within the Perdew-Burke-Ernzerhof (PBE) scheme [32]. We used a mesh cutoff of 500 Ry for real-space integrals and a double- ζ polarized basis to ensure good convergence. Atomic forces were relaxed to a tolerance of 0.005 eV/Å using molecular dynamics. The edges of these dimer systems were passivated with hydrogen atoms. Mulliken analysis confirmed that the total spin of S-1T is equal to \hbar , while the total spins of S-1/2T and S-1/2O are $\hbar/2$.

TABLE I. Bilinear and biquadratic exchange constants for the dimer systems depicted in Fig. 1.

Dimer Coupling	J (meV)	β
(a)	15.7	0.02
(b)	38.4	0.08
(c)	48.8	0.08
(d)	24.4	0.04
(e)	27.5	0.04
(f)	43.2	0.08

The second step is to compute the bilinear and biquadratic exchange constants of the Hamiltonian in Eq. 1 in the context of the magnetic force theorem and the LKAG formalism [33–35] using the electronic Hamiltonian previously computed as input, as explained in more detail in Ref. [36]. These exchange parameters are obtained by mapping to the classical

version of Eq. 1, where spin operators are replaced by unit vectors. Therefore, Table I compiles the exchange parameters for the different dimer systems shown in Fig. 1, excluding the S factors. Notice that all isotropic exchange couplings favor antiferromagnetic (AFM) alignments between the two spins. Throughout this work, we assume exchange interactions between the MBBs exist only among nearest neighbors [25, 36, 37]. Moreover, to avoid undesired contributions to the exchange parameters, we have projected the magnetic entities onto the $2p_z$ -orbitals [38], which are responsible for the magnetism in these zigzag-edged nanographene structures [39, 40]. The reported values for the exchange coupling J between two S-1/2O [23], two S-1/2T [24], and two S-1T [25] are 38, 45, and 18 meV, respectively. These values are in good agreement with the theoretical results we report in Table I(a-c).

Lastly, the third step is to perform Exact Diagonalization (ED) on the Hamiltonian \hat{H}_{BLBQ} given by Eq. 1 using the exchange parameters previously obtained. Since the operators \hat{H}_{BLBQ} , $\hat{S}_T^2 = (\sum_i \hat{\mathbf{S}}_i)^2$ and $\hat{S}_T^z = \sum_i \hat{S}_i^z$

commute with each other, the eigenstates of \hat{H}_{BLBQ} labelled by λ can be characterized with the respective quantum numbers S and M and are computed using ED. As we will see in section III B, for certain eigenstates a degeneracy not related to these quantum numbers emerges that is related to an additional symmetry of \hat{H}_{BLBQ} .

III. RESULTS

A. Alternating spin-1 and spin-1/2 chains

The theory of alternating quantum spin chains has been studied for more than 60 years [41–45]. In their seminal work, Lieb and Mattis [41] presented significant analytical results for bipartite spin systems described by a quantum AFM isotropic Heisenberg Hamiltonian. In the particular case of bipartite chains, the spin species in each sublattice may not be equal; for example, one sublattice may consist of spin-1 and the other of spin-1/2. When this occurs, we refer to it as an alternating spin chain. The Lieb-Mattis theorem [41] can be applied to an alternating AFM spin chain as follows. Suppose that the exchange interaction occurs only between the first nearest neighbors, and let \mathcal{S}_A (\mathcal{S}_B) denote the maximum possible spin on sublattice A (B). According to the theorem, the quantum spin number S for the ground state (GS) of the system is given by $S = |\mathcal{S}_A - \mathcal{S}_B|$. For an alternating spin-1 and spin-1/2 of length N the spin of the GS will be given by

$$S = \lfloor N/2 \rfloor + \text{mod}(N, 2) - 0.5 \lfloor N/2 \rfloor, \quad (2)$$

where $\lfloor \cdot \rfloor$ is the floor function. This reflects the net magnetization as a function of N and the ferrimagnetic

behavior, as S grows linearly with N . The degeneracy $g = 2S + 1$ of the ground state is also linearly dependent on N . It has been shown that the ground state differs from the ferrimagnetic Néel state due to quantum fluctuations [43]. Although these results are for zero biquadratic interaction, this interaction does not affect the rotational invariance of the Hamiltonian, and therefore, Eq. 2 still holds as we have confirmed in our ED simulations. Later, we will show that the biquadratic interaction only affects the energy gap of the GS.

In this paper, we propose to use MBBs such as S-1T, S-1/2T or S-1/2O to construct an alternating quantum spin chain as depicted in Fig. 2(a). These chains are described by a simplified form of Eq. 1

$$\hat{H}_{\text{chain}} = \sum_i J \left(\hat{\mathbf{S}}_i \cdot \hat{\mathbf{S}}_{i+1} + \beta \left(\hat{\mathbf{S}}_i \cdot \hat{\mathbf{S}}_{i+1} \right)^2 \right). \quad (3)$$

Based on the results mentioned above, we show that by engineering such a system, the ground state exhibits ferrimagnetic behavior, with both the spin number S and the degeneracy of the GS depending on the length of the chain. At the top of Fig. 2(a), we depict an alternating spin-1 and spin-1/2 chain composed of S-1T and S-1/2T, while at the bottom, the chain is composed of S-1T and S-1/2O. Different types of alternating spin chains can be constructed using different MBBs, such as aza-triangulenes ([46, 47]) or larger triangulenes with higher spin moment. The isotropic and biquadratic exchange constants J and β for these chains are given in Table I. In Fig. 2(b), we show the energy gap to the first excited state as a function of N in blue. In the limit of infinite chain length, the energy gap vanishes [42]. The total spin S of the GS is shown in red as a function of N , confirming that it follows Lieb's theorem, as given in Eq. 2. The variation in the energy gap values plotted in Figure 2(b) differs by approximately 2% when a biquadratic interaction $\beta = 0.04$ is not included.

B. Three-Leg Spin Graphs

When a spin system cannot be divided into sublattices, as in the case of 3-LSG, Lieb's theorem [41] is no longer applicable. To the best of our knowledge, there is no theorem or result that could predict the ground state of the Hamiltonian given by Eq. 1 as a function of the couplings and spin constituents.

We will devote this section to study 3-LSG whose MBBs are either S-1T or S-1/2T, respectively. We will perform ED on Eq. 1 for three different 3-LSG lengths, $N=7, 10$, and 13 spin-1 and spin-1/2 sites, as depicted in Fig. 3. In Table II, we compile the total spin quantum number for the GS and the first excited state (ES), as well as the energy gap between them, for the six 3-LSGs. We find that the first ES is two-fold degenerate in energy

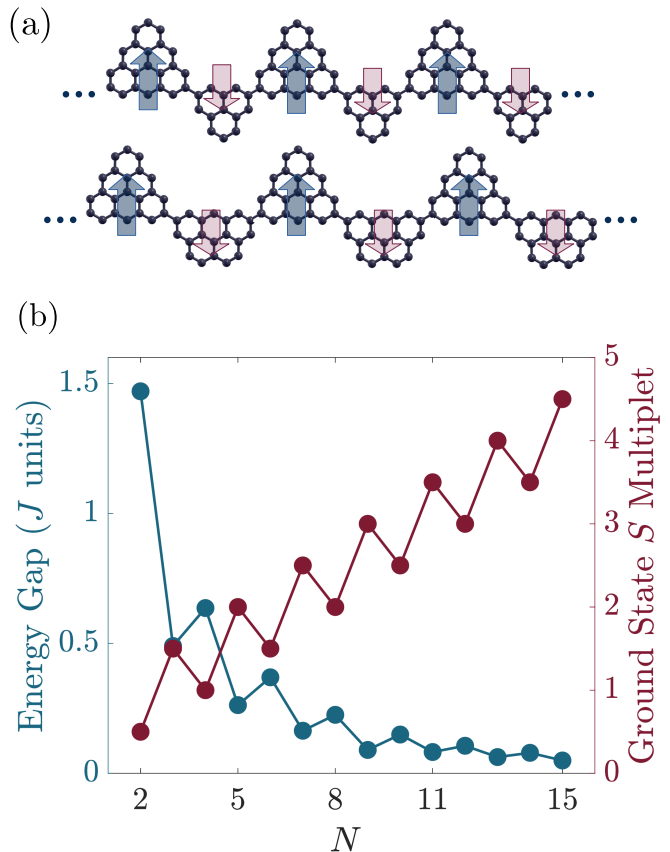


FIG. 2. (a) shows the two types of ferrimagnetic alternating spin-1 and spin-1/2 chains that can be formed from different graphene MBBs. The top chain is made from S-1T and S-1/2T MBBs, while the bottom chain is made from S-1T and S-1/2O MBBs. Blue (red) arrows represent spin-1 (spin-1/2) sites. (b) shows the energy gap between the GS and the first excited state in blue, and the quantum spin number S for the GS in red, as a function of the chain length N . Both calculations were performed using ED over Eq. 3 taking $\beta=0.04$.

and spin S quantum number. We will refer to this as double- S degeneracy. For example, for a $N = 10$ 3-LSG made by spin-1 MBBs, the first ES is composed by two-fold degenerate $S = 1$ states which gives a total of degenerate six states (two $M = -1$, two $M = 0$ and two $M = 1$ states). Moreover, following this case, in the presence of a magnetic field represented by the Zeeman term, $H_Z = -B\hat{S}_T^z$, the ES will have $M = 1$ while remaining two-fold degenerate.

This phenomenon is common to all six 3-LSGs studied in this section for different MBBs and is robust for different β values in the range $[0, 0.1]$ within the same phase. As far as we know, we have not found any other spin systems in the literature where degenerate eigenstates of the Hamiltonian have the same S and M quantum numbers, with other words, the eigenstates of \hat{H} can not be unequivocally classified with S and M . We will address this issue later in this section.

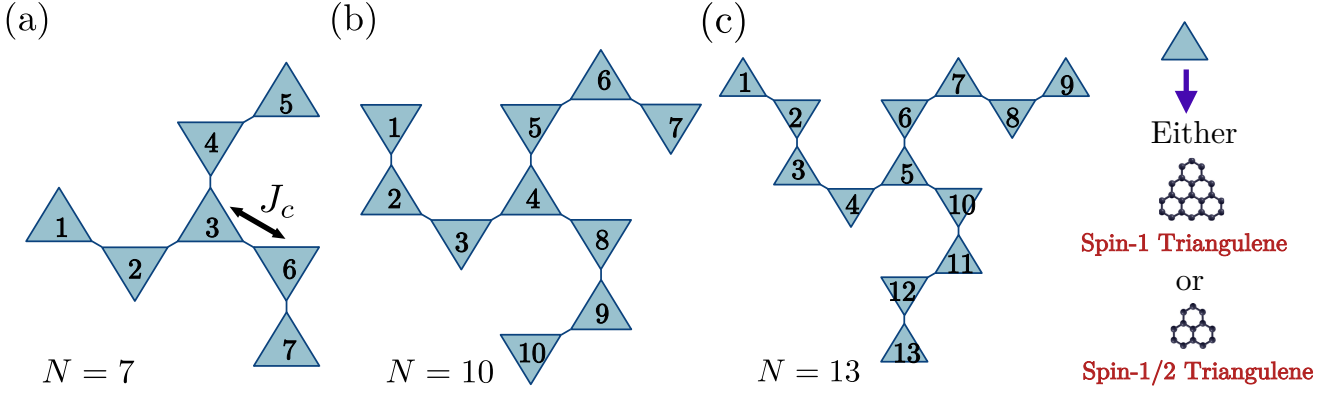


FIG. 3. (a-c) 3-LSGs of lengths $N = 7, 10$, and 13 MBBs, respectively. Each blue triangle either represents a spin-1 or spin-1/2 MBB (S-1T or S-1/2T), coupled via isotropic and biquadratic exchange interactions between nearest neighbors (see Table I). Site labels are shown in black for the $N = 7, 10$, and 13 3-LSGs. For $N = 7$, J_c denotes the isotropic exchange coupling between sites 3 and 6.

TABLE II. S value for the GS and the two-fold degenerate first ES, computed via ED using the Hamiltonian in Eq. 1, for a 3-LSG composed of either spin-1 or spin-1/2 MBBs of varying lengths ($N = 7, 10$ and 13). The energy gap between the GS and ES is also provided.

3-LSG	GS	ES	Gap (J units)
$N = 7$, spin-1/2	$S = 1/2$	$S = 1/2$	0.72
$N = 7$, spin-1	$S = 1$	$S = 0$	0.60
$N = 10$, spin-1/2	$S = 1$	$S = 0$	0.27
$N = 10$, spin-1	$S = 2$	$S = 1$	0.40
$N = 13$, spin-1/2	$S = 1/2$	$S = 1/2$	0.46
$N = 13$, spin-1	$S = 1$	$S = 0$	0.27

To understand how the double- S degeneracy arises, we focus on the $N = 7$ 3-LSG composed of spin-1 MBBs, where the isotropic exchange coupling J_c connects sites 3 and 6, as shown in Fig. 3(a). When $J_c = 0$ the system consists of two uncoupled spin-1 chains: one of length $N = 5$ and the other of length $N = 2$. The GS of an open spin-1 chain depends on the number of sites [36, 48–50], being a singlet (triplet) if the number of sites is even (odd). Thus, for the $N = 2$ chain, the GS and ES are a singlet ($S_{N=2} = 0$) and triplet ($S_{N=2} = 1$), respectively, while for the $N = 5$ chain, the GS and ES are reversed, being a triplet ($S_{N=5} = 1$) and singlet ($S_{N=5} = 0$), respectively. Fig. 4(a) illustrates how the eigenvalues of the Hilbert space, formed by the $N = 2$ and $N = 5$ chains, are combined through the tensor product. The GS is a triplet, arising from $S_{N=5} = 1$ and $S_{N=2} = 0$, while the first ES is a singlet, formed by $S_{N=5} = 0$ and $S_{N=2} = 0$. The second ES consists of a singlet, a triplet, and a quintuplet, resulting from the combination of the two triplets, $S_{N=5} = 1$ and $S_{N=2} = 1$. Figs. 4(b–d) illustrate how the singlet, formed by the combination of $S_{N=5} = 1$ and $S_{N=2} = 1$, decreases in energy as the exchange coupling J_c increases, approaching the singlet ES. The energy difference between the first and second singlet

ESs for $J_c = 0.2J$ ($J_c = 0.8J$) is approximately 40% (8%). When $J_c = J$, both singlets become degenerate giving rise to the double- S degeneracy. The degeneracy mechanism shown in Figs. 4(a–d) is valid only for the $N = 7$ 3-LSG with spin-1 MBBs. However, an analogous description applies to the other 3-LSGs listed in Table II.

As what follows we show that the Hamilton operator of three-leg spin graphs exhibits a symmetry that leads to double degeneracies of some ESs. We first introduce the swap operator, which has been widely used in quantum computing [51, 52], but not in theoretical magnetism. Suppose an operator \hat{A} composed by a tensorial product of three operators \hat{A}_1 , \hat{A}_2 and \hat{A}_3 acting on different Hilbert spaces \mathcal{H}_1 , \mathcal{H}_2 and \mathcal{H}_3 spanned by $\{|v_1\rangle \dots |v_{N_v}\rangle\}$, $\{|u_1\rangle \dots |u_{N_u}\rangle\}$ and $\{|w_1\rangle \dots |w_{N_w}\rangle\}$, respectively. This reads

$$\begin{aligned} \hat{A} &= \hat{A}_1 \otimes \hat{A}_2 \otimes \hat{A}_3 = \\ &= \sum A_{v\tilde{v}}^1 A_{u\tilde{u}}^2 A_{w\tilde{w}}^3 |v\rangle \langle \tilde{v}| \otimes |u\rangle \langle \tilde{u}| \otimes |w\rangle \langle \tilde{w}| \end{aligned} \quad (4)$$

where we omitted to present the indices in the sums for simplicity. The unitary operator that swaps the order in the tensor product of the second and third operators in Eq. (4) is given by

$$\hat{U}_{23} = \hat{\mathcal{I}}_1 \otimes \sum (|\tilde{u}\rangle \langle \tilde{w}| \otimes |w\rangle \langle u|) \quad (5)$$

where $\hat{\mathcal{I}}_1$ is the identity operator acting on \mathcal{H}_1 . It can be readily proven that $\hat{U}_{23} \hat{A} \hat{U}_{23}^\dagger = \hat{A}_1 \otimes \hat{A}_3 \otimes \hat{A}_2$. A general form of the swap operator that exchanges i th and j th spaces in $\mathcal{H}_1 \otimes \mathcal{H}_2 \otimes \dots \otimes \mathcal{H}_N$ is given by the following expression

$$\hat{U}_{ij} = \sum_{ij} \hat{\mathcal{I}}_1 \otimes \hat{\mathcal{I}}_2 \otimes \dots \otimes |i\rangle \langle j| \otimes \dots \otimes |j\rangle \langle i| \otimes \dots \otimes \hat{\mathcal{I}}_N \quad (6)$$

where $|i\rangle = \{|i_1\rangle, \dots, |i_{N_i}\rangle\}$ and $|j\rangle = \{|j_1\rangle, \dots, |j_{N_j}\rangle\}$ span \mathcal{H}_i and \mathcal{H}_j , respectively. It can be immediately seen that \hat{U}_{ij} is unitary $\hat{U}_{ij} \hat{U}_{ij}^\dagger = \hat{U}_{ij}^\dagger \hat{U}_{ij} =$

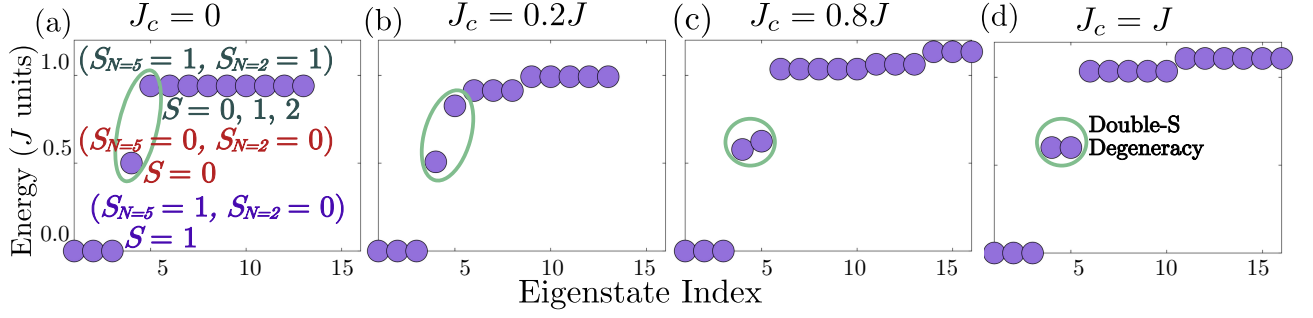


FIG. 4. (a-d) ED calculations based on the Hamiltonian given by Eq. 1 for an $N = 7$ three-leg spin graph composed of spin-1 MBs. The exchange coupling J_c connects sites three and six, following the labeling in Fig. 3 (a), thereby coupling two chains: one with $N = 2$ and the other with $N = 5$. As J_c increases, the two singlet states circled in green - one in the first ES and the other in the second ES - progressively approach each other in energy until they become degenerate at $J_c = J$.

$$\hat{I}_1 \otimes \cdots \otimes \hat{I}_i \otimes \cdots \otimes \hat{I}_j \otimes \cdots \otimes \hat{I}_N.$$

We have realized that 3-LSGs possess swapping transformations that leave \hat{H}_{BLBQ} invariant. For example, the operator \hat{U}_N^{C+} that generates an cyclic swapping transformation, namely, an anticlockwise rotation of the legs on a 3-LSG of N sites can be constructed as a product of the swapping operators given in Eq. (6):

$$\hat{U}_{N=7}^{C+} = \hat{U}_{6,4} \hat{U}_{2,6} \hat{U}_{7,5} \hat{U}_{1,7} \quad (7)$$

$$\hat{U}_{N=10}^{C+} = \hat{U}_{5,8} \hat{U}_{3,5} \hat{U}_{6,9} \hat{U}_{2,6} \hat{U}_{7,10} \hat{U}_{1,7} \quad (8)$$

$$\hat{U}_{N=13}^{C+} = \hat{U}_{6,10} \hat{U}_{4,6} \hat{U}_{7,11} \hat{U}_{3,7} \hat{U}_{8,12} \hat{U}_{2,8} \hat{U}_{9,13} \hat{U}_{1,9}. \quad (9)$$

where the labeling of the sites in the 3-LSG is described in Fig. 3. \hat{U}_N^{C+} is a unitary operator that commutes with \hat{H}_{BLBQ} , \hat{S}_T^2 and \hat{S}_T^z . Clearly, the adjoint of \hat{U}_N^{C+} , i.e., the clockwise rotation \hat{U}_N^{C-} , also commutes with the Hamiltonian. Moreover, the combination of swapping operators that interchange two legs in 3-LSGs also leaves the Hamiltonian invariant. We will denote them by $\hat{U}_N^{\sigma I}$, where $I = 1, 2, 3$ labels the leg which is unaffected by the symmetry transformation.

Consequently, there exist six swapping symmetry transformations $\{\hat{U}_N^I, \hat{U}_N^{C+}, \hat{U}_N^{C-}, \hat{U}_N^{\sigma 1}, \hat{U}_N^{\sigma 2}, \hat{U}_N^{\sigma 3}\}$, where \hat{U}_N^I stands for the identity transformation. These transformations form a group G_N , which is isomorphic to the C_{3v} point group. The multiplication table of the group elements can easily be checked, and, as an example, a visual representation of the product $\hat{U}_N^{\sigma 3} \hat{U}_N^{\sigma 1} = \hat{U}_N^{C-}$ is shown in Fig. 5.

The group G_N has then two one-dimensional and one two-dimensional irreducible representations, A_1 , A_2 and E , respectively. As well-known from representation theory, the eigenstates of the Hamiltonian can be classified according to the irreducible representations. For the case $N = 7$ 3-LSG of spin-1, we numerically checked that the three eigenstates with lowest energy correspond to the one-dimensional total symmetric A_1 representation, i.e., they remain invariant upon any swapping symmetry transformation. The degeneracy of these states is then

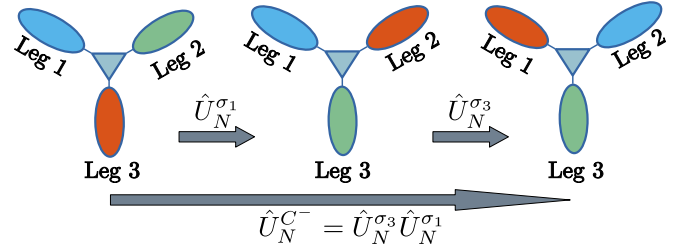


FIG. 5. The construction of the cyclic swapping transformation \hat{U}_N^{C-} for a 3-LSG is illustrated as a subsequent action of the transformation $\hat{U}_N^{\sigma 3}$ and $\hat{U}_N^{\sigma 1}$. Colors indicate the different spin operators associated with the legs.

clearly due to the $M = 0, \pm 1$ quantum numbers of the triplet ($S = 1$) spin-state. On the contrary, by applying the symmetry transformations the two states of the first ES transformed into their linear combinations. It was, however, possible to find a unitary transformation of these two states such that the representation of the symmetry transformations recovered the well-established two-by-two matrices of the E irreducible representation [53]. This unambiguously proved that the two-fold degeneracy of the first ES of 3-LSGs is dictated by the swapping symmetry of the Hamiltonian. It is also clear that the six-fold degenerate fourth ES with $S = 1$ of the $N = 7$ 3-LSG, see Fig. 4(d), also corresponds to the E irreducible representation.

The expectation values of \hat{S}_i^z for the GS and the first ES are shown in Fig. 6 for an $N = 7$ 3-LSG of spin-1/2 MBs. Notice that $\langle \hat{S}_i^z \rangle$ takes the same values for the tuples 1-5-7 and 2-4-6 due to the C_3 swapping symmetry given by Eq. 7. In Fig. 6(a), the GS exhibits a large value of $\langle \hat{S}_i^z \rangle$ at the edges ($i = 1, 5$, and 7). Conversely, in Fig. 6(b), the ES shows the opposite behavior, with values close to zero. This behavior of greater localization for the GS and less for the ES is general for the chains studied in this section, except for the singlet states, for which the expectation value of \hat{S}_i^z is zero. On the other hand, the correlator between i and j sites

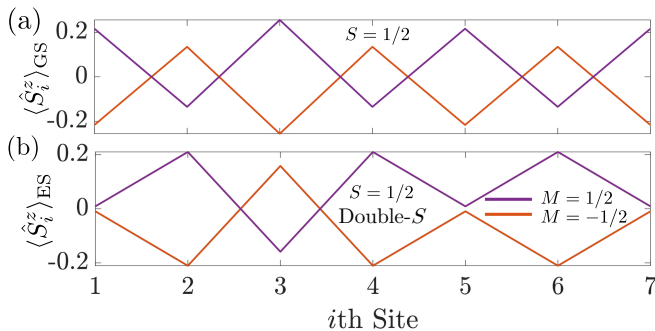


FIG. 6. (a) and (b) show the expectation value $\langle \hat{S}_i^z \rangle$ for the GS and the first ES, respectively, for an $N = 7$ 3-LSG composed of S-1/2Ts. In (b) the ES is composed by four states $|\lambda_{\text{ES}}, S = 1/2, M = \pm 1/2\rangle$ because it is double-S degenerate. The labeling of the spin sites is given by Fig. 3.

defined as $\mathcal{L}_{ij} = \langle \hat{\mathbf{S}}_i \cdot \hat{\mathbf{S}}_j \rangle - \langle \hat{\mathbf{S}}_i \rangle \cdot \langle \hat{\mathbf{S}}_j \rangle$ gives us useful information about the GS and the ES. The maximum correlation between the edges $|\mathcal{L}_{17}|$ of the previous 3-LSG for the state $|\lambda_{\text{GS}}, S = 1/2, M = 1/2\rangle$ reaches a value of 9% of $S(S+1)$, while for the state $|\lambda_{\text{ES}}, S = 1/2, M = 1/2\rangle$, the value of $|\mathcal{L}_{17}|$ reaches 30% of $S(S+1)$. From this result, we can conclude that the edges in the 3-LSG are more correlated for the ES than for the GS. For the case of an $N = 13$ 3-LSG of spin-1/2 MBBs, the correlation between edges is much smaller than that for the $N = 7$ case. It is that $|\mathcal{L}_{1(13)}|$ is approximately a 4% of $S(S+1)$ for the $|\lambda_{\text{GS}}, S = 1/2, M = 1/2\rangle$ state and $|\mathcal{L}_{1(13)}|$ is approximately a 17% of $S(S+1)$ for the $|\lambda_{\text{ES}}, S = 1/2, M = 1/2\rangle$ state. Thus, the correlation between edges is shown to decay more strongly as the length of the legs of the 3-LSG increases, as expected [42, 43, 54].

The results presented in this section regarding the double-S degeneracy are general for any spin system described by H_{BLBQ} , provided that the couplings and spin species are equivalent to those of the 3-LSGs.

IV. SUMMARY AND CONCLUSIONS

We compute the bilinear and biquadratic exchange constants for various dimer systems composed of different magnetic nanographene structures combining three different first-principles approaches. DFT [29–31] calculations are used to obtain the electronic Hamiltonian, then the LKAG formalism [33–35] enables us to extract the exchange constants from Eq. 1. Last but not least, ED method [27] computes gaps in the energy spectrum and the quantum numbers of the eigenstates. We propose a theoretical realization of alternating spin-1 and spin-1/2 chains composed of different MBBs, such as S-1T, S-1/2T, and S-1/2O. These alternating chains exhibit ferrimagnetism, and both the total quantum spin S and the GS degeneracy scale linearly with the length of the chain. We then characterize the low-energy eigenstates of 3-LSGs of varying lengths ($N = 7, 10$, and 13 MBBs)

and compositions (either S-1T or S-1/2T). In the first ES, we identify a double degeneracy in the total spin quantum number S . We showed that this unexpected feature of the spectrum arises due to the symmetry of the Hamiltonian with respect to swapping transformations that form a group which is isomorphic to the C_{3v} point group. The identification of symmetry-induced degeneracies in 3-LSGs highlights the potential relevance of such symmetries in other quantum systems governed by Hamiltonians with analogous structural properties. These findings open new avenues for the experimental design of custom spin graphs using magnetic building blocks (MBBs). They also lay the groundwork for exploring quantum degeneracies dictated by discrete spatial symmetries in engineered nanostructures. Moreover, since the results presented in this paper rely on ED calculations of the BLBQ Hamiltonian, they can be generalized to physical systems beyond those based on nanographene structures, provided that the spin species and couplings are similar to those considered in this work.

ACKNOWLEDGEMENTS

G. M.-C., A. G.-F. and J. F. have been funded by Ministerio de Ciencia, Innovación y Universidades, Agencia Estatal de Investigación, Fondo Europeo de Desarrollo Regional via the grants PGC2018-094783 and PID2022-137078NB-I00, and by Asturias FICYT under grant AYUD/2021/51185 and by Agencia SEKUENS (Asturias) under grant UONANO IDE/2024/000678 with the support of FEDER funds. G. M.-C. has been supported by Programa “Severo Ochoa” de Ayudas para la investigación y docencia del Principado de Asturias. This work was supported by the Ministry of Culture and Innovation and the National Research, Development and Innovation Office within the Quantum Information National Laboratory of Hungary (Grant No. 2022-2.1.1-NL-2022-00004) and projects K131938, K142179 ADVANCED 149745. We thank the “Frontline” Research Excellence Programme of the NRDIO, Grant No. KKP133827. This project has received funding from the HUN-REN Hungarian Research Network. This project is supported by the TRILMAX Horizon Europe consortium (Grant No. 101159646).

Appendix A: Multi-leg and mixed spin graphs

In this appendix, we present several examples of structures built from S-1T, S-1/2T, and S-1/2O. The possible combinations of these spin-1 and spin-1/2 MBBs, incorporating different couplings and varying lengths, make this field a vast playground for study, where the properties of both the GS and ES are highly sensitive to the structural configuration. Some examples of all these possibilities are shown in Fig. 7 and Table III presents the S values for the GS and ES, along with the energy gap,

for those structures.

Fig. 7(a) depict modifications of the 3-LSGs presented in the previous section, where the central triangulene species differs from that of the legs. The 3-LSG shown in Fig. 7(a) exhibits a two-fold degenerate singlet ES, similar to those studied in Table II.

Figs. 7(b–c) show examples of possible four-leg spin graphs composed of S-1T, S-1/2T, and S-1/2O as MBBs. Finally, Fig. 7(d) shows an example of a six-leg spin graph (6-LSG) made from S-1/2Ts. This 6-LSG also possesses a C_3 swapping symmetry, and notably, its first excited state is a double- S with $S = 1$. In contrast, for a

similar 6-LSG in which the spin-1/2 MBBs are replaced by S-1Ts the ground state will be a $S = 4$ and the first excited state will be a double- S with $S = 3$. Larger combinations of MBBs can form nanostructures with an arbitrary number of legs.

TABLE III. S values for the GS and the first ES computed by ED, as well as the energy gap between them, for the spin graphs depicted in Fig. 7.

System	GS	ES	Gap (meV)
(a)	$S = 1$	$S = 0$ (two-fold deg.)	25.9
(b)	$S = 1/2$	$S = 1/2$	17.6
(c)	$S = 0$	$S = 1$	14.9
(d)	$S = 2$	$S = 1$ (two-fold deg.)	7.8

- [1] R. Garreis, C. Tong, J. Terle, M. J. Ruckriegel, J. D. Gerber, L. M. Gächter, K. Watanabe, T. Taniguchi, T. Ihn, K. Ensslin, and W. W. Huang, Long-lived valley states in bilayer graphene quantum dots, *Nature Physics* **20**, 428 (2024).
- [2] I. Alonso Calafell, J. D. Cox, M. Radonjić, J. R. M. Saavedra, F. J. García de Abajo, L. A. Rozema, and P. Walther, Quantum computing with graphene plasmons, *npj Quantum Information* **5**, 37 (2019).
- [3] Y. Zhang, R. Polski, A. Thomson, É. Lantagne-Hurtubise, C. Lewandowski, H. Zhou, K. Watanabe, T. Taniguchi, J. Alicea, and S. Nadj-Perge, Enhanced superconductivity in spin-orbit proximitized bilayer graphene, *Nature* **613**, 268 (2023).
- [4] M. Oh, K. P. Nuckolls, D. Wong, R. L. Lee, X. Liu, K. Watanabe, T. Taniguchi, and A. Yazdani, Evidence for unconventional superconductivity in twisted bilayer graphene, *Nature* **600**, 240 (2021).
- [5] J. Lehmann, A. Gaita-Ariño, E. Coronado, and D. Loss, Quantum computing with molecular spin systems, *Journal of Materials Chemistry* **19**, 1672 (2009).
- [6] A. Signoles, T. Franz, R. Ferracini Alves, M. Gärttner, S. Whitlock, G. Zürn, and M. Weidemüller, Glassy dynamics in a disordered heisenberg quantum spin system, *Phys. Rev. X* **11**, 011011 (2021).
- [7] E. A. Stepanov, S. Brener, F. Krien, M. Harland, A. I. Lichtenstein, and M. I. Katsnelson, Effective heisenberg model and exchange interaction for strongly correlated systems, *Phys. Rev. Lett.* **121**, 037204 (2018).
- [8] L. M. Gächter, R. Garreis, J. D. Gerber, M. J. Ruckriegel, C. Tong, B. Kratochwil, F. K. de Vries, A. Kurzmann, K. Watanabe, T. Taniguchi, T. Ihn, K. Ensslin, and W. W. Huang, Single-shot spin readout in graphene quantum dots, *PRX Quantum* **3**, 020343 (2022).
- [9] Q. H. Wang, A. Bedoya-Pinto, M. Blei, A. H. Dismukes, A. Hamo, S. Jenkins, M. Koperski, Y. Liu, Q.-C. Sun, E. J. Telford, H. H. Kim, M. Augustin, U. Vool, J.-X. Yin, L. H. Li, A. Falin, C. R. Dean, F. Casanova, R. F. L. Evans, M. Chshiev, A. Mishchenko, C. Petrovic, R. He, L. Zhao, A. W. Tsien, B. D. Gerardot, M. Brotons-Gisbert, Z. Guguchia, X. Roy, S. Tongay, Z. Wang, M. Z. Hasan, J. Wrachtrup, A. Yacoby, A. Fert, S. Parkin, K. S. Novoselov, P. Dai, L. Balicas, and E. J. G. Santos, The magnetic genome of two-dimensional van der waals materials, *ACS Nano* **16**, 6960 (2022).
- [10] B. Huang, G. Clark, E. Navarro-Moratalla, D. R. Klein, R. Cheng, K. L. Seyler, D. Zhong, E. Schmidgall, M. A. McGuire, D. H. Cobden, W. Yao, D. Xiao, P. Jarillo-Herrero, and X. Xu, Layer-dependent ferromagnetism in a van der waals crystal down to the monolayer limit, *Nature* **546**, 270 (2017).
- [11] C. Boix-Constant, A. Rybakov, C. Miranda-Pérez, G. Martínez-Carracedo, J. Ferrer, S. Mañas-Valero, and E. Coronado, Programmable magnetic hysteresis in orthogonally-twisted 2d crsbr magnets via stacking engineering., *Advanced Materials* **37**, 2415774 (2025), 2415774.
- [12] G. Martínez-Carracedo, A. García-Fuente, L. Oroszlány, L. Szunyogh, and J. Ferrer, Tuning magnetic exchange interactions in two-dimensional magnets: The case of CrGeX_3 ($x = \text{se, te}$) and janus $\text{cr}_2\text{ge}_2(\text{se,te})_3$ monolayers, *Phys. Rev. B* **110**, 184406 (2024).
- [13] R. Hanson, L. P. Kouwenhoven, J. R. Petta, S. Tarucha, and L. M. K. Vandersypen, Spins in few-electron quantum dots, *Rev. Mod. Phys.* **79**, 1217 (2007).
- [14] M. H. Appel, A. Ghorbal, N. Shofer, L. Zaporski, S. Manna, S. F. C. da Silva, U. Haeusler, C. Le Gall, A. Rastelli, D. A. Gangloff, and M. Atatüre, A many-body quantum register for a spin qubit, *Nature Physics* **21**, 368 (2025).
- [15] S. Zuo, J. Liu, K. Qiao, Y. Zhang, J. Chen, N. Su, Y. Liu, J. Cao, T. Zhao, J. Wang, F. Hu, J. Sun, C. Jiang, and B. Shen, Spontaneous topological magnetic transitions in ndco5 rare-earth magnets, *Advanced Materials* **33**, 2103751 (2021).
- [16] F. Tejo, R. H. Heredero, O. Chubykalo-Fesenko, and K. Y. Guslienko, The bloch point 3d topological charge induced by the magnetostatic interaction, *Scientific Reports* **11**, 21714 (2021).
- [17] S. Fujii and T. Enoki, Nanographene and graphene edges: Electronic structure and nanofabrication, *Accounts of Chemical Research* **46**, 2202 (2013).
- [18] S. Cheng, Z. Xue, C. Li, Y. Liu, L. Xiang, Y. Ke, K. Yan, S. Wang, and P. Yu, On-surface synthesis of triangu-

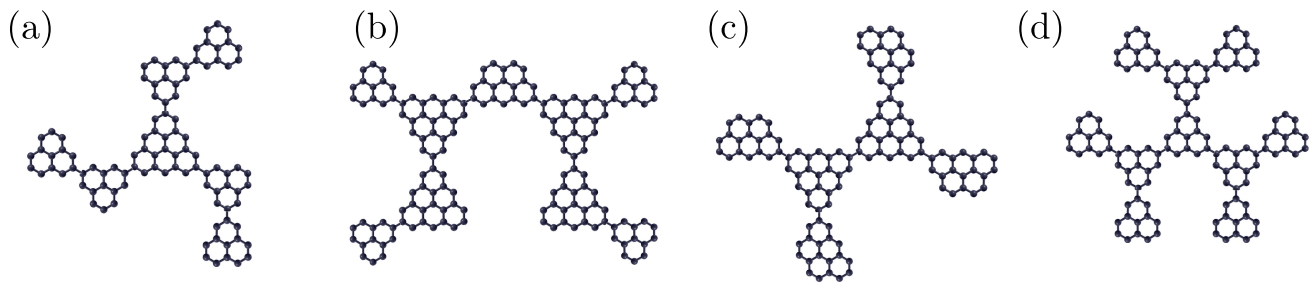


FIG. 7. (a) 3-LSG combining S-1T and S-1/2T MBBs. (b-c) Various four-leg spin graphs incorporating S-1T, S-1/2O, and S-1/2T MBBs. (d) Six-leg graph made from S-1/2T.

- lene trimers via dehydration reaction, *Nature Communications* **13**, 1705 (2022).
- [19] S. Song, A. Pinar Solé, A. Matěj, G. Li, O. Stetsovych, D. Soler, H. Yang, M. Telychko, J. Li, M. Kumar, Q. Chen, S. Edalatmanesh, J. Brabec, L. Veis, J. Wu, P. Jelinek, and J. Lu, Highly entangled polyradical nanographene with coexisting strong correlation and topological frustration, *Nature Chemistry* **16**, 938 (2024).
- [20] G. Z. Magda, X. Jin, I. Hagymási, P. Vancsó, Z. Osváth, P. Nemes-Incze, C. Hwang, L. P. Biró, and L. Tapasztó, Room-temperature magnetic order on zigzag edges of narrow graphene nanoribbons, *Nature* **514**, 608 (2014).
- [21] E. H. Lieb, Two theorems on the hubbard model, *Phys. Rev. Lett.* **62**, 1201 (1989).
- [22] S. Mishra, D. Beyer, K. Eimre, J. Liu, R. Berger, O. Gröning, C. A. Pignedoli, K. Müllen, R. Fasel, X. Feng, and P. Ruffieux, Synthesis and characterization of π -extended triangulene, *Journal of the American Chemical Society* **141**, 10621 (2019).
- [23] C. Zhao, L. Yang, J. C. G. Henriques, M. Ferri-Cortés, G. Catarina, C. A. Pignedoli, J. Ma, X. Feng, P. Ruffieux, J. Fernández-Rossier, and R. Fasel, Spin excitations in nanographene-based antiferromagnetic spin-1/2 heisenberg chains, *Nature Materials* 10.1038/s41563-025-02166-1 (2025).
- [24] Z. Yuan, X.-Y. Zhang, Y. Jiang, X. Qian, Y. Wang, Y. Liu, L. Liu, X. Liu, D. Guan, Y. Li, H. Zheng, C. Liu, J. Jia, M. Qin, P.-N. Liu, D.-Y. Li, and S. Wang, Fractional spinon quasiparticles in open-shell triangulene spin-1/2 chains, *Journal of the American Chemical Society* **147**, 5004 (2025).
- [25] S. Mishra, G. Catarina, F. Wu, R. Ortiz, D. Jacob, K. Eimre, J. Ma, C. A. Pignedoli, X. Feng, P. Ruffieux, J. Fernández-Rossier, and R. Fasel, Observation of fractional edge excitations in nanographene spin chains, *Nature* **598**, 287 (2021).
- [26] J. C. G. Henriques and J. Fernández-Rossier, Anatomy of linear and nonlinear intermolecular exchange in $s = 1$ nanographene, *Phys. Rev. B* **108**, 155423 (2023).
- [27] P. Nataf and F. Mila, Exact diagonalization of heisenberg $SU(n)$ models, *Phys. Rev. Lett.* **113**, 127204 (2014).
- [28] M. Wu, D.-X. Yao, and H.-Q. Wu, Exact diagonalization study of the anisotropic heisenberg model related to $ybmga_4$, *Phys. Rev. B* **103**, 205122 (2021).
- [29] P. Hohenberg and W. Kohn, Inhomogeneous electron gas, *Phys. Rev.* **136**, B864 (1964).
- [30] W. Kohn and L. J. Sham, Self-consistent equations including exchange and correlation effects, *Phys. Rev.* **140**, A1133 (1965).
- [31] J. M. Soler, E. Artacho, J. D. Gale, A. García, J. Junquera, P. Ordejón, and D. Sánchez-Portal, The siesta method for ab initio order-n materials simulation, *Journal of Physics: Condensed Matter* **14**, 2745 (2002).
- [32] J. P. Perdew, K. Burke, and M. Ernzerhof, Generalized gradient approximation made simple, *Phys. Rev. Lett.* **77**, 3865 (1996).
- [33] A. I. Liechtenstein, M. I. Katsnelson, V. P. Antropov, and V. A. Gubanov, Local spin density functional approach to the theory of exchange interactions in ferromagnetic metals and alloys, *Journal of Magnetism and Magnetic Materials* **67**, 65 (1987).
- [34] L. Udvardi, L. Szunyogh, K. Palotás, and P. Weinberger, First-principles relativistic study of spin waves in thin magnetic films, *Phys. Rev. B* **68**, 104436 (2003).
- [35] L. Oroszlány, J. Ferrer, A. Deák, L. Udvardi, and L. Szunyogh, Exchange interactions from a nonorthogonal basis set: From bulk ferromagnets to the magnetism in low-dimensional graphene systems, *Phys. Rev. B* **99**, 224412 (2019).
- [36] G. Martínez-Carracedo, L. Oroszlány, A. García-Fuente, L. Szunyogh, and J. Ferrer, Electrically driven singlet-triplet transition in triangulene spin-1 chains, *Phys. Rev. B* **107**, 035432 (2023).
- [37] Y. Saleem, T. Steenbock, E. R. J. Alhadi, W. Pasek, G. Bester, and P. Potasz, Superexchange mechanism in coupled triangulenes forming spin-1 chains, *Nano Letters* **24**, 7417 (2024).
- [38] G. Martínez-Carracedo, L. Oroszlány, A. García-Fuente, B. Nyári, L. Udvardi, L. Szunyogh, and J. Ferrer, Relativistic magnetic interactions from nonorthogonal basis sets, *Phys. Rev. B* **108**, 214418 (2023).
- [39] J. Fernández-Rossier and J. J. Palacios, Magnetism in graphene nanoislands, *Phys. Rev. Lett.* **99**, 177204 (2007).
- [40] Y. Ominato and M. Koshino, Orbital magnetism of graphene nanostructures, *Solid State Communications* **175-176**, 51 (2013).
- [41] E. Lieb and D. Mattis, Ordering energy levels of interacting spin systems, *Journal of Mathematical Physics* **3**, 749 (1962), https://pubs.aip.org/aip/jmp/article-pdf/3/4/749/19167430/749_1.online.pdf.
- [42] S. K. Pati, S. Ramasesha, and D. Sen, Low-lying excited states and low-temperature properties of an alternating spin-1–spin-1/2 chain: A density-matrix renormalization-group study, *Phys. Rev. B* **55**, 8894 (1997).

- [43] S. Brehmer, H.-J. Mikeska, and S. Yamamoto, Low-temperature properties of quantum antiferromagnetic chains with alternating spins and, *Journal of Physics: Condensed Matter* **9**, 3921 (1997).
- [44] A. E. Trumper and C. Gazza, Antiferromagnetically coupled alternating spin chains, *Phys. Rev. B* **64**, 134408 (2001).
- [45] H. Wu, G. Wei, A. Du, G. Yi, and W. Gong, Exact results of an alternating-bond mixed spin-1/2 and spin-1 ising chain with both longitudinal and transverse single-ion anisotropies, *Journal of Magnetism and Magnetic Materials* **323**, 1428 (2011).
- [46] T. Wang, A. Berdonces-Layunta, N. Friedrich, M. Vilas-Varela, J. P. Calupitan, J. I. Pascual, D. Peña, D. Casanova, M. Corso, and D. G. de Oteyza, Aza-triangulene: On-surface synthesis and electronic and magnetic properties, *Journal of the American Chemical Society* **144**, 4522 (2022).
- [47] M. Vilas-Varela, F. Romero-Lara, A. Vegliante, J. P. Calupitan, A. Martínez, L. Meyer, U. Uriarte-Amiano, N. Friedrich, D. Wang, F. Schulz, N. E. Koval, M. E. Sandoval-Salinas, D. Casanova, M. Corso, E. Artacho, D. Peña, and J. I. Pascual, On-surface synthesis and characterization of a high-spin aza-[5]-triangulene, *Angewandte Chemie International Edition* **62**, e202307884 (2023).
- [48] F. D. M. Haldane, Continuum dynamics of the 1-d heisenberg antiferromagnet: Identification with the o(3) non-linear sigma model, *Physics Letters A* **93**, 464 (1983).
- [49] I. Affleck, T. Kennedy, E. H. Lieb, and H. Tasaki, Rigorous results on valence-bond ground states in antiferromagnets, *Phys. Rev. Lett.* **59**, 799 (1987).
- [50] B. Jaworowski, N. Rogers, M. Grabowski, and P. Hawrylak, Macroscopic singlet-triplet qubit in synthetic spin-one chain in semiconductor nanowires, *Scientific Reports* **7**, 5529 (2017).
- [51] J. Siewert, On orthogonal bases in the hilbert-schmidt space of matrices, *Journal of Physics Communications* **6**, 055014 (2022).
- [52] M. A. Nielsen and I. L. Chuang, *Quantum Computation and Quantum Information: 10th Anniversary Edition* (Cambridge University Press, Cambridge, 2010).
- [53] S. L. Altmann and P. M. Herzig, Point-group theory tables (1994).
- [54] Y. J. Kim, M. Greven, U.-J. Wiese, and R. J. Birgeneau, Monte-carlo study of correlations in quantum spin chains at non-zero temperature, *The European Physical Journal B - Condensed Matter and Complex Systems* **4**, 291 (1998).